J Mater Sci: Mater Electron (2021) 32:15386–15392

Flexible zinc oxide photoelectrode for photo electrochemical energy conversion

T. Shiyani[1], I. Banerjee[1], Santosh K. Mahapatra[2], and Asim K. Ray[3,*]

[1] School of Nanosciences, Central University of Gujarat, Gandhinagar 382030, Gujarat, India
[2] School of Physical Sciences, Central University of Punjab, Bathinda 151001, Punjab, India
[3] Brunel University, Uxbridge, London, UK

Received: 16 March 2021
Accepted: 28 April 2021
Published online: 18 May 2021

ABSTRACT

Photoelectrochemical properties have been investigated for flexible photoelectrodes containing 310 nm thick ZnO film on spin-coated ITO/PET. The high crystalline structure of ZnO was studied using x-ray diffraction pattern. A value of 3.4 eV has been estimated for optical band gap from its absorption spectra. The flexible ZnO photoelectrode was demonstrated to generate photoelectrochemical current. The photocurrents are enhanced by 4% whereas flat-band potential is shifted by 8 V due to the illumination. Values of 1.022 and 0.714 AW^{-1} were found to be for photo switching and photoresponsivity, respectively. ZnO/ITO/PET can be used as a substrate for making flexible hybrid PEC devices to generate solar power and solar fuels.

1 Introduction

Photoelectrochemical (PEC) cells are one type of solar cells that include photoelectrodes and electrolyte [1]. Photoelectrodes can be fabricated from various materials including organic and inorganic materials. The materials of photoelectrodes decide the performance of PECs [2]. Semiconducting photoelectrodes are mostly used in PECs for conversion of photons into electron–hole pairs [3]. First PEC was demonstrated using TiO_2. Thereafter, many nanostructured metal oxides have been used in PECs because the advantages of high surface to volume ratio in nanomaterials [4].

Zinc oxide (ZnO) is a n-type semiconducting material with a wide direct energy band gap with a value of 3.37 eV at room temperature [5]. Values of 3.96×10^{20} cm^{-3} and 17.7 cm^2V^{-1} s^{-1} have been reported for electron concentration and mobility of co-doped RF sputtered ZnO films. Optical transmission value is similar to 85–90% in the range 400–700 nm for these films [6]. Because of its low toxicity and high electronic conductivity, it has been extensively studied for exploring applications in optoelectronics as solar cells, gas sensors, varistors and a phosphor for colour displays [7]. The On–Off ratio as high as 2.2×10^4 has been reported for the ZnO memristor in a sandwich configuration with sputtered gold top electrode [8].

Flexible photo-electrochemical cells of ZnO on indium tin oxide (ITO) coated polyethylene terephthalate (PET) substrates, incorporating muga silk

Address correspondence to E-mail: asim.ray@brunel.ac.uk

https://doi.org/10.1007/s10854-021-06088-x

nanoparticles of sizes ranging between 28 nm - 142 nm have been recently studied under white light illumination of power 56 $mWcm^{-2}$. The value of photoresponsivity is found to be 0.119 μAW^{-1}. The rise time is 0.9 s while the corresponding decay time is 0.6 s [9]. Similarly configured photo-electrochemical cells using basil sensitized ZnO show 0.45% energy conversion efficiency. The photocurrent and photovoltage were enhanced by 1.33 nA and 3 mV, respectively. Values of 1.3 and 0.024 µA/W have been reported for On–Off ratio and photoresponsivity, respectively [10]. Flexible Ultraviolet zinc nanorods photodetectors are reported to show photoresponsivity within the range of 0.13–0.19 A/W under UV power density varying between 0.8 and 12.47 $mWcm^{-2}$ [11]. ZnO films drop-cast on fluorine doped ITO substrates was coated with a layer of natural dye for hybrid photoelectrodes with improved performance [12]. The dye-sensitised solar cells have been fabricated using natural dye extracted from basil or *ocimum* leaves. These may also be used as photo-electrochemical cell for the applications of water splitting [13]. This article presents the photochemical properties of 310 nm thick spin coated ZnO films using commercially available nanoparticles.

2 Experimental details

2.1 Materials and device fabrication

ZnO thin films were deposited on ITO coated PET substrates (purchased from Sigma Aldrich) with prior cleaning through spin coating technique. Small volume of 40 weight% dispersion of ZnO nanoparticles (130 nm) dispersed in ethanol was spin coated on ITO/PET substrate at 250 rpm and 2000 rpm in a sequence for 15 s and 60 s respectively. The samples were kept for oven drying at 60 °C for 15 min [14, 15].

2.2 Characteriation techniques

X-Ray diffraction (XRD) patterns were acquired using a Bruker D8 Advance scanning in the 2θ range of 5–1001, with a step size of 0.021 per second using CuKα radiation of wavelength 0.15406 nm. ITO coated PET substrate was used for the UV–Visible. The absorption and transmittance spectra were recorded using UV–Visible spectrophotometer (Shimadzu 6120, Japan). The photoelectrochemical (PEC) measurements were performed in a standard three electrode configuration using Scanning electrochemical microscopy (SECM, CH Instrument, model CHI920D) as shown in Fig. 1. ZnO film was used as working electrode, a saturated calomel electrode (SCE) was used as reference and a Pt wire was used as counter electrode in a standard three electrode system with 0.1 M Na_2SO_4 aqueous solution as electrolyte. The fabricated ZnO/ITO/PET device was converted into photoelectrode and used as working electrode in PEC cell. The linear sweep voltametry technique was used at scan rate of 0.1 V/s. The white LED light (with intensity of about 56 mW/cm^2) was used as light source to measure current–voltage (I-V) behavior of the PEC cell under dark and light [16, 17].

3 Result and Discussion

3.1 Structural properties of ZnO/ITO thin film

XRD pattern of ZnO thin film grown on ITO-PET substrate is shown in Fig. 2. XRD experiments were performed with X-ray diffractometer. XRD pattern was used to study the orientation and phase of the sample. The marked diffraction peaks are corresponding to ZnO. The (101) peak at 2θ = 33.58° was observed, which corresponds ZnO (JCPDS card No.

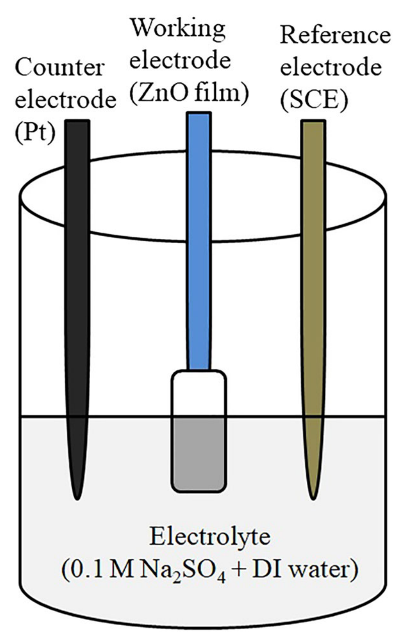

Fig. 1 Schematic representation of three electrode electrochemical system

89–1397) corresponding to the hexagonal wurtzite structure of ZnO. The two diffraction peaks at 47° and 54.6° that are corresponding to the ITO-PET substrate. The XRD pattern confirms ZnO film with high crystallinity.

3.2 Optical properties

The absorption spectra of ZnO thin film deposited on ITO coated PET substrate were measured by the UV–Visible spectrometer in the wavelength range 200–1100 nm as shown in Fig. 3a. The absorption curve shows the absorption peak about 387 nm for ZnO thin film. The optical band gap of the films was determined using the Tauc plot as shown in Fig. 3b. The obtained band gap was found about 3.4 eV for the ZnO thin film. The various optical parameters of ZnO/ITO/PET device are summarized in Table 1. The transmittance of the film was very high due to transparent behavior of film as shown in Fig. 3c. The Urbach curve is shown in Fig. 3d and Urbach energy is found at 0.2890 eV.

3.3 Refractive index calculation

ZnO film exhibits good transparency in the visible and infrared region (∼ 78%). The refractive index (*n*) at different wavelengths was calculated using the envelope curve method in the transmission spectra [18]. The equation for refractive index is expressed as Eq. (1). Values of refractive index n for ZnO film are found to be 2.0506 and 2.0501 at 492 nm and 802 nm wavelengths, respectively from Eq. (1).

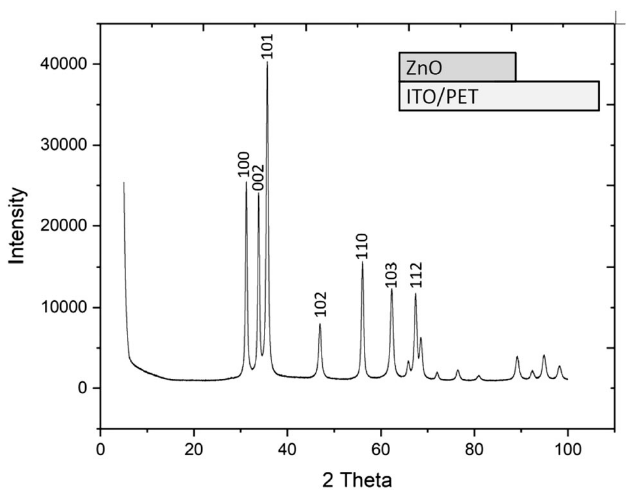

Fig. 2 X-ray diffraction patern of ZnO/ITO/PET. The inset shows the device structure

$$n = \left[N + (N^2 - n_s^2)^{1/2}\right]^{1/2} \quad (1)$$

where N = 2 ns $[(T_M - T_m)/T_M T_m] + (n_s^2 + 1)/2$ and n_s is refractive index of substrate. The values of refractive index are consistent with those reported recently [18].

3.4 Thickness calculation

The thickness of the ZnO film was calculated using the Eq. (2) [19]. The thickness of ZnO film was found as 310 nm.

$$t = (\lambda_1 \lambda_2)/[2(\lambda_1 n_2 - \lambda_2 n_1)] \quad (2)$$

where n_1 and n_2 are the refractive indices corresponding to wavelengths λ_1 and λ_2, respectively.

3.5 Urbach energy calculation

The exponential dependence on the photon energy ($h\upsilon$) by the absorption coefficient (α) near the band edge for noncrystalline materials follows the Urbach relation as expressed in Eq. (3). Urbach curve shows the variation in the logarithm of the absorption coefficient as a function of the photon energy for ZnO film. The value of Urbach energy (*Eu*) is normally calculated by considering the reciprocal of the slope of the linear portion in the lower photon energy region of these curves [20]. The calculated values of Urbach energy for ZnO film is about 0.2890 eV.

$$\alpha(\upsilon) = \alpha_0 \exp(h\upsilon/E_u) \quad (3)$$

where α_0 is a constant, *Eu* is an energy which is interpreted as the width of the tail of localized states in the forbidden band gap, υ is the frequency of radiation, and *h* is Planck's constant. The value of 0.2890 eV for Urbach energy is believed to be relative to the degree of crystallinity in the spin-coated ZnO [21]

Values of optical parameters in Table 1 are consistent with published data [22]

3.6 Photoelectrochemical properties

The energy band diagram of ZnO/ITO/PET is shown in Fig. 4, which explains the charge transfer mechanism in PEC device. The photo electrochemical (PEC) response of the ZnO/ITO/PET with Na_2SO_4 electrolyte was recorded using linear sweep photovoltammogram and photoamperometric technique as

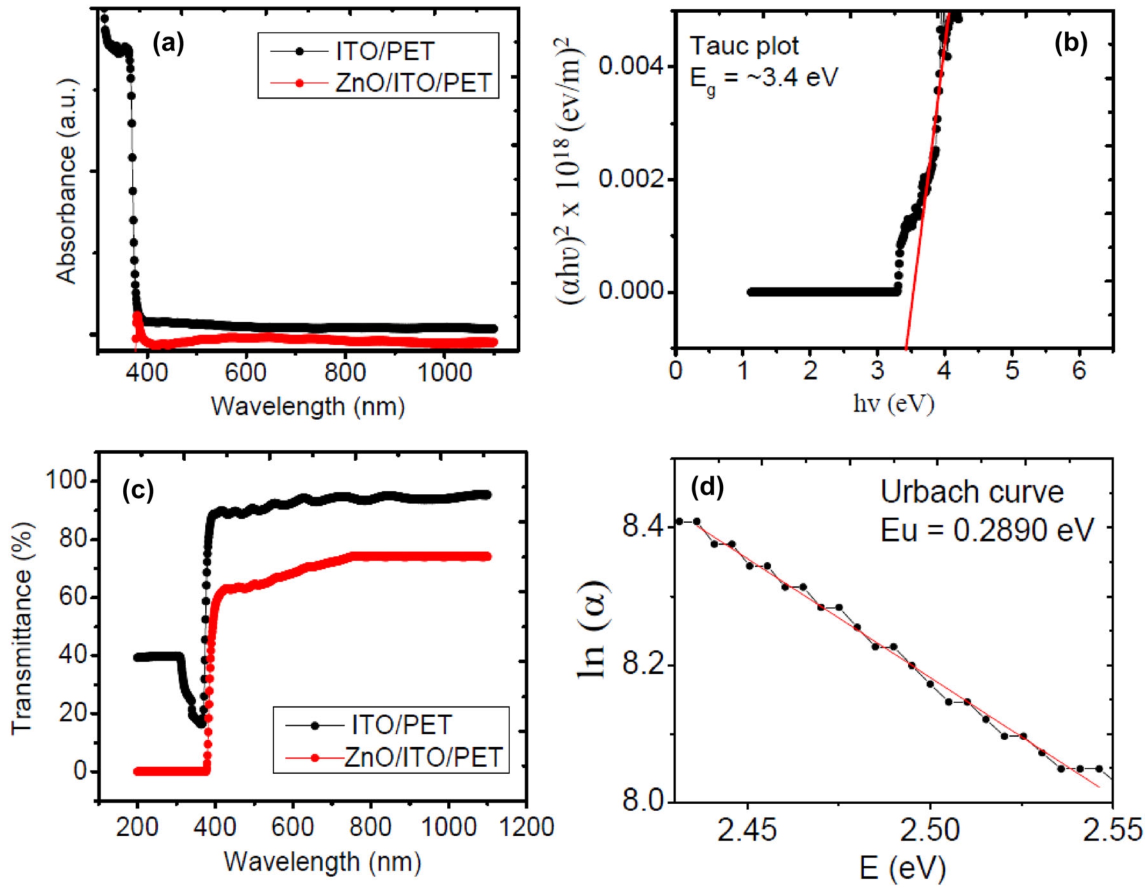

Fig. 3 **a** Absorbance spectra, **b** Tauc plot **c** Transmittance spectra, **d** Urbach curve of ZnO/ITO/PET

Table 1 Optical parameters of ZnO/ITO/PET

Device	Band gap (eV)	Refractive index (n)		Urbach energy (E_u) eV
		n at 492 nm	n at 802 nm	
ZnO/ITO/PET	3.4	2.0506	2.0501	0.2890

shown in Fig. 5 and 6, respectively. The dark and red color is shown for without illumination and under illumination, respectively. The PEC response confirms that the film was photoactive film. A negative slope of I-V shows the n-type semiconducting behavior of ZnO. At high photon energy, the maximum photovoltage dimishes due to the limited penetration depth of ZnO. Then excited electron enters into the ZnO region and diffuses at back contact. As a result, there is a generation of photocurrent and photo voltage. The photo generated carriers are collected due to the electric field present at the semiconductor-electrolyte interface. The photocurrent is directly dependent on the properties of semiconductor layer [23]

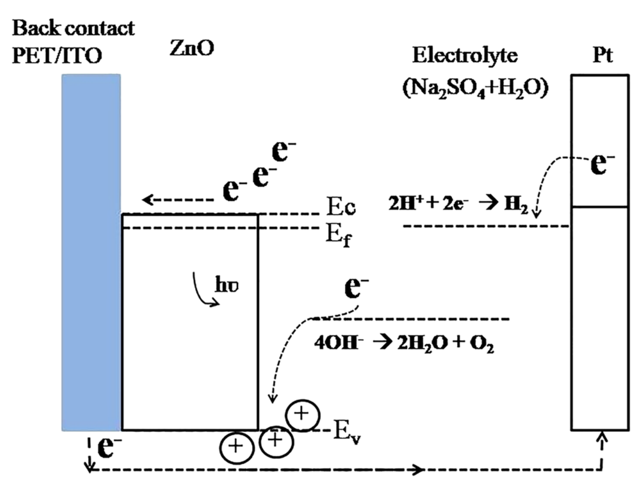

Fig. 4 A schematic of electron flow in photo electrochemical cell

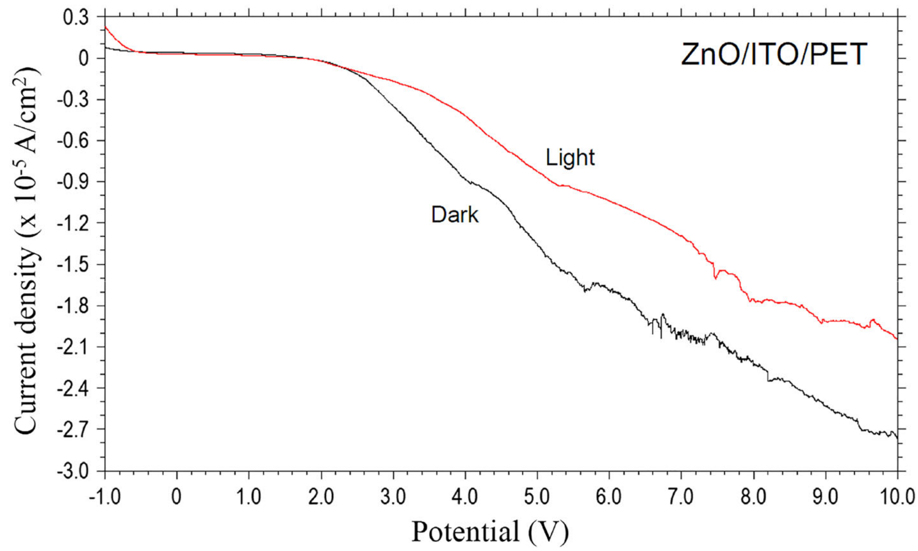

Fig. 5 Linear Sweep voltametry of ZnO/ITO/PET in dark (black) and light (red)

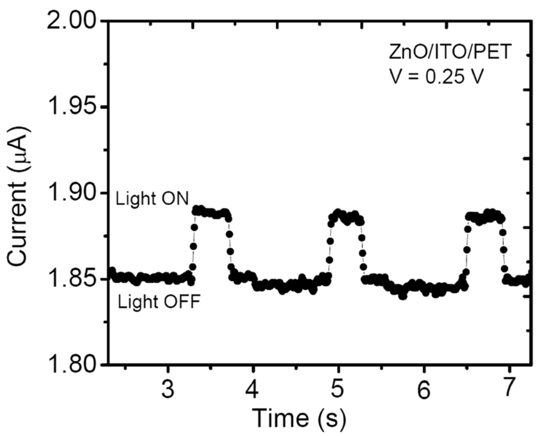

Fig. 6 Photoamperometric at 0.25 V of ZnO/PET

The I-V curves show the flat-band potential V_{FB}. It is the potential where there is no field in the semiconductor) shifts towards the negative values, which shows n-type behavior of semiconducting thin film in PEC device. The flat band potential was shifted towards higher value under illumination from 2.6 V to 3.4 V. In the photoamperometric measurement, the working electrode is held at a constant 0.25 V potential and illuminated with white LED light for a short period of time. The photocurrent was observed at 1.85 μA and 1.89 μA for dark and illuminated condition, respectively. The photocurrent is enhanced by 4% and flat-band potential increased by 0.8 V due to the illumination. The flexible ZnO photoelectrode was demonstrated for photoswitching properties and photoresponsive behavior. The ON/OFF ratio and photoresponsivity were calculated about 1.0216 and 0.7142 μA/W, respectively. The measured photoelectrochemical parameters are summarized in Table 2.

ZnO can only absorb ultraviolet (UV) light (4% in the sun light spectrum) due to its wide band gap [20]. Therefore, ZnO photoelectrodes can be modified with organic or inorganic materials to absorb visible and other spectrum of sun light. Biomaterials have high absorption in visible spectrum. Natural dyes can absorb the light in a wide range of wavelengths. Flexible ZnO/ITO/PET photoelectrodes can be used as a substrate for developing next generation hybrid solar energy conversion devices as well as wearable optoelectronic devices. [24].

4 Conclusions

We have demonstrated flexible ZnO photoelectrode for photoelectrochemical solar energy conversion. The flexible thin film solar cells have greater advantages for commercial productions because of their flexibility and lightweight features. Flexible ZnO PEC device has generated photocurrents of about 1.85 μA and 1.89 μA under dark and illumination, respectively. The flat band potential was shifted from 2.6 to 3.4 V due to the illumination. The photocurrents and flat-band potential are enhanced by 4% and 0.8 V, respectively due to the illumination. The flexible ZnO/ITO/PET has shown photoswitching ON/OFF ratio and photoresponsivity about 1.0216 and 0.7142 μA/W, respectively. These results provide a fundamental understanding on flexible ZnO

Table 2 Photoelectrochemical parameters for flexible ZnO photoelectrode

Device	Photocurrent (μA)		V_F (V)		Increment due to illumination		ON/OFF ratio (I_{Light}/I_{Dark})	Photoresponsivity R(AW^{-1})
	Dark	Light	Dark	Light	Photocurrent	V_F (V)		
ZnO/ITO	1.85	1.89	2.6	3.4	4%	0.8	1.0216	0.714 AW^{-1}

photoelectrode and can be used to develop hybrid solar cells for generation of solar power as well as solar fuels.

Acknowledgements

The authors are thankful to Central Instrumentation Facility (CIF), Central University of Gujarat for providing scanning electrochemical microscope facility.

Declarations

Conflict of interest The authors declare no conflict of interest.

References

1. R.N. Clayton, The earth and the sun. Science **332**(6037), 1509–1510 (2011)
2. B. O'Regan, A low-cost, high-efficiency solar cell based on dye-sensitized colloidal TiO2 films. Nature **353**, 737–740 (1991)
3. M. Gratzel, Photoelectrochemical cells. Nature **414**, 338 (2001)
4. T. Shiyani, T. Bagchi, Hybrid nanostructures for solar energy conversion applications. Nanomater. Energy **9**(1), 1–8 (2020)
5. P.P. Ortega, C.C. Silva, M.A. Ramirez, G. Biasotto, C.R. Foschini, A.Z. Simoes, Multifunctional environmental applications of ZnO nanostructures synthesized by the microwave-assisted hydrothermal technique. Appl. Surf. Sci. **542**, 148723 (2021)
6. J.S. Wu, D.F. Xue, Progress of Science and Technology of ZnO as Advanced Material. Sci. Adv. Mater. **3**(2), 127–149 (2011)
7. S. Ghosh, A. Mallick, B. Dou, F.A.M. Van Hest Maikel, S.M. Garner, D. Basak, A novel blanket annealing process to achieve highly transparent and conducting Al doped ZnO thin films Its mechanism and application in perovskite solar cells. Sol. Energy **174**, 815–825 (2020)
8. S. Paul, P.G. Harris, C. Pal, A.K. Sharma, A.K. Ray, Low cost zinc oxide for memristors with high On-Off ratios. Mater. Lett. **130**, 40–42 (2014)
9. P.C. Asapur, T. Shiyani, S.K. Mahapatra, K.A. Bogle, I. Banerjee, Photo-electrochemical property of microwave synthesized muga silk nanoparticles/ZnO/ITO/PET Structure *IETE Tech*. Rev. (2020). https://doi.org/10.1080/02564602.2020.1852121
10. T. Shiyani, S.K. Mahapatra, I. Banerjee, Basil sensitized ZnO photoelectrochemical cell for solar energy conversion. Mater. Today **32**(3), 412–416 (2020)
11. L. Ghorbani, S. Nasirian, Zinc oxide nanorods assisted by polyaniline network as a flexible self-powered Ultraviolet photodetector: a comprehensive study. Appl. Surf. Sci. **527**, 146786 (2020)
12. T. Shiyani, S. Agrawal, I. Banerjee, Natural dye sensitized photo electrochemical cells for solar energy conversion. Nanomaterials and Energy **9**(2), 1–9 (2020)
13. T. Shiyani, S. K. Mahapatra, and I. Banerjee, Natural basil as photosensitizer with ZnO thin films for solar cell applications, IETE Journal of Research, pp. 1–8 (2020). Doi: https://doi.org/10.1080/03772063.2020.1768161.
14. E. Muchuweni, T.S. Sathiaraj, H. Nyakotyo, Synthesis and characterization of zinc oxide thin films for optoelectronic applications. Heliyon **3**(4), e00285 (2017)

15. S. Choudary et al., International journal of modern physics: conference series. World Scientific Publishing Company **22**, 545–551 (2013). https://doi.org/10.1142/S2010194513010647
16. W. Wang, T. Ai, Yu. Qi, Electrical and photocatalytic properties of boron-doped ZnO nanostructure grown on PET–ITO flexible substrates by hydrothermal method. Sci. Rep. **7**, 42615 (2017)
17. M. Gupta, V. Sharma, J. Shrivastava, A. Solanki, Preparation and characterization of nanostructured ZnO thin films for photoelectrochemical splitting of water. Bull. Mater. Sci. **32**(1), 23–30 (2009)
18. M. Caglar, Y. Caglar, S. Ilican, The determination of the thickness and optical constants of the ZnO crystalline thin film by using envelope method. J. Optoelectron. Adv. Mater. **8**(4), 1410–1413 (2006)
19. H.E. Ali, V. Ganesh, L. Haritha, A.M. Aboraia, H.H. Hegazy, V. Butova, A.V. Soldatov, H. Algarni, A. Guda, H.Y. Zahran, Kramers-Kronig analysis of the optical linearity and nonlinearity of nanostructured Ga-doped ZnO thin films. Opt. Laser Technol. **135**, 106691 (2021)
20. S. Asha, Y. Sangappa, S. Ganesh, Tuning the Refractive Index and Optical Band Gap of Silk Fibroin Films by Electron Irradiation. J. Spectroscopy **2015**, 1–7 (2015)
21. F. Urbach, The long-wavelength edge of photographic sensitivity and of the electronic absorption of solids. Phys. Rev. **92**, 1324 (1953)
22. E. Przezdziecka, K.M. Paradowska, A. Lysak, A. Wierzbicka, P. Sybilski, E. Placzek-Popko, R. Jakiela, J.M. Sajkowski, A. Kozanecki, Influence of As doping on the properties of nonpolar ZnO. Thin Solid Films **720**, 138520 (2021)
23. N. Wang, D.Y. Jiang, Light trapping in ZnO nanowires to control ultraviolet photodetection responsivity. J. Mater. Sci. **56**(9), 5708–5716 (2021)
24. R. Dom, S. Govindarajan, S.V. Joshi, P.H. Borse, A solar-responsive zinc oxide photoanode for solar-photon-harvester photoelectrochemical (PEC) cells. Nanoscale Adv. **2**, 3350 (2020)